Polymerization

Deutsche Ausgabe: DOI: 10.1002/ange.201602485
Internationale Ausgabe: DOI: 10.1002/anie.201602485

Of Poisons and Antidotes in Polypropylene Catalysis

*Yue Yu, Vincenzo Busico, Peter H. M. Budzelaar, Antonio Vittoria, and Roberta Cipullo**

Abstract: *Quenched-flow studies of $MgCl_2$-supported Ziegler–Natta catalysts were combined for the first time with ^{13}C NMR fingerprinting of the nascent polymer and conclusively proved that, depending on the catalyst formulation, propene polymerization can be slowed down significantly by the occurrence of the few regiodefects (2,1 monomer insertions), changing active sites into dormant sites. Catalysts modified with ethylbenzoate show little dormancy. The more industrially relevant phthalate based catalysts, instead, are highly dormant and require the presence of H_2 to counteract the deleterious effect of this self-poisoning on productivity and stereoselectivity.*

Isotactic polypropylene (i-PP) is the second largest volume polymer on the market after polyethylene, and the current production of 60 MT/*y* is almost entirely based on $MgCl_2$-supported titanium-based catalysts of the Ziegler–Natta (ZN) type.[1] The active forms of these systems are obtained by the interaction of a $MgCl_2/TiCl_4$/ID precatalyst (ID = internal donor) with an AlR_3 or AlR_3/ED cocatalyst (ED = external donor; Table 1).[2–4] It is generally agreed that the active sites are inherently chiral alkylated titanium(III) species,[2–6] but their number and structure(s) are uncertain.

Table 1: Typical formulations and performance of $MgCl_2$-supported ZN catalyst systems for i-PP.[3]

ID	ED	Productivity[a]	AF[b]	M_w/M_n
ethylbenzoate	aromatic monoester	15–30	4–7	8–10
dialkylphthalate	alkoxysilane	40–70	1–5	6–8
2,2′-dialkyl-1,3-dimethoxypropane	none or alkoxysilane	70–100	1–2	4–5
dialkylsuccinate	alkoxysilane	40–70	1–5	10–15

[a] Kg(PP) g(catalyst)$^{-1}$. [b] PP amorphous fraction (AF) in wt%.

Catalyst productivity is the product of the fraction of the active titanium (x^*) and average chain propagation constant (k_p). One way to estimate x^* in a ZN catalyst is to count how many polymer chains are growing at a given time. This has been done by means of quenched flow (QF) methods[7–10] in the short (< 1 s) initial transient time period of controlled kinetics, during which chain-transfer and termination processes are still negligible.[11] The conclusion was that x^* is low (between 1 and 10%),[7–10] but whether this holds at later stages of the polymerization is unclear. Alternatively, the growing chains can be labeled with radioactive tags (such as ^{14}CO or CH_3OT); this approach yielded somewhat larger x^* values (up to 20%),[12–14] but the underlying chemistry is delicate, and the possibility of multiple tagging[15] or partial inclusion of aluminum-bound chains in the count cannot be ruled out.

That only a relatively small part of $TiCl_4$ is converted into a catalytic species is plausible. According to the literature, activation entails alkylation by AlR_3, followed by homolytic cleavage of the Ti^{IV}–R bond.[2–4,16] Redox titrations concluded that the process is complex, and yields a distribution of titanium oxidation states, with residual Ti^{IV}, and comparable amounts of Ti^{III} and Ti^{II}.[2,3,17,18] The majority of the Ti^{III} species are EPR silent; this behavior has been traced to the formation of aggregates.[2–4,17–19] In this respect, one should recall that the reaction of $TiCl_4$ with alkyl–aluminum compounds in hydrocarbon solution ultimately leads to the precipitation of crystalline $TiCl_3$, which is a moderately active and largely EPR-silent heterogeneous propene polymerization catalyst.[3,4,20] On the other hand, a very recent high-resolution EPR investigation of an activated fourth-generation industrial catalyst found that about 10% of the total titanium in this catalyst is EPR-active, and the hyperfine structure of the spectra is compatible with isolated molecular-like Ti^{III} surface adducts.[18] It is tempting to identify (part of) the latter with the catalytic species. In such a hypothesis, the strong dependence of catalyst performance on the used ID/ED pair (Table 1) can be explained assuming that ID and/or ED molecules, co-adsorbed at close contact, modulate the steric and electronic properties of the active metal, similar to ancillary ligands in molecular catalysts.[6,21,22] The concept is simple and elegant, but has not yet been translated into well-defined and generally accepted structural models.

To learn more on these elusive systems, we combined for the first time the standard QF approach[7–10] with a thorough ^{13}C NMR fingerprinting[6] of the nascent polymer, including a quantitative determination of the chain ends; this is now made possible by the superior sensitivity of the novel NMR high-temperature cryoprobes.[23,24] Our aim, in particular, was to shed light onto the complex and partly controversial molecular kinetic picture of Scheme 1.[6] It is well-known that, in general, ZN catalysts are highly regioselective in favor of 1,2 propene insertion ($k_{ps} \approx 10^{-3}\ k_{pp}$ in Scheme 1).[2–4,6,25–27] On the other hand, there are reasons to believe that propene insertion into the Ti–CH(Me)–CH_2(R) species formed by occasional 2,1 insertions is extremely slow ($k_{sp} \ll k_{pp}$, $k_{ss} \approx 0$ in Scheme 1).[25–27] This low rate may lead to an accumulation of

[*] Dr. Y. Yu, Prof. Dr. V. Busico, M. Sc. A. Vittoria, Prof. Dr. R. Cipullo
Department of Chemical Sciences
Federico II University of Naples
Complesso di Monte S. Angelo, Via Cintia, 80126 Napoli (Italy)
E-mail: rcipullo@unina.it
Prof. Dr. P. H. M. Budzelaar
Department of Chemistry, University of Manitoba
144 Dysart Road—Winnipeg, Manitoba R3T 2N2 (Canada)
Supporting information and the ORCID identification number(s) for the author(s) of this article can be found under http://dx.doi.org/10.1002/anie.201602485.

 © 2016 Wiley-VCH Verlag GmbH & Co. KGaA, Weinheim

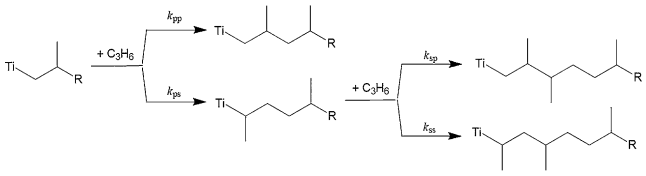

Scheme 1. Formation and further reaction of secondary alkyl–titanium species.

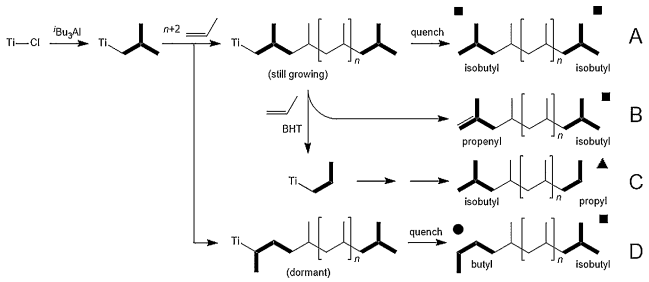

Scheme 2. Formation of initial and terminal PP chain ends. The ■, ▲, and ● labels are for structure identification in Figure 2. BHT = 3,5-di-*tert*-butyl-4-hydroxytoluene.

dormant chains in the system, and possibly represent an important (if not the main) cause of the low x^* value. The hypothesis rests on solid but circumstantial evidence. In particular, it relies on educated guesses of the relative reactivity of primary and secondary alkyl–titanium species with H_2 or ethene, and in the former case the data mainly refers to the regiochemistry of low-molar-mass PP fractions (hydro-oligomers[28]). As such, it has not received a general endorsement.[4,29,30]

Full details of our approach (with related protocols) are provided in the Supporting Information. The first system that we looked at consisted of a $MgCl_2/TiCl_4$/EB precatalyst (EB = ethylbenzoate)[2–4] in combination with Al(*i*Bu)$_3$ (TIBA).[31] Now of lesser industrial relevance, this has been the catalyst of choice for QF investigations because of a very fast chain initiation.[7–10] The results of a series of QF propene polymerization experiments at 30 °C in a heptane slurry and a reaction time (t) in the 0–0.5 second range are reported in Table SI-1 (see the Supporting Information). A short induction period was observed in the polymer yield versus time plot (see Figure SI-2), and once the induction was over (indicatively, at $t > 0.1$ s), both the polymer yield and the number average polymerization degree (P_n) increased linearly with time. The best-fit values of the main kinetic parameters, obtained by interpolation of the $\{Y, t\}$ and $\{P_n^{-1}, t^{-1}\}$ data sets, as discussed in Section SI-5.1, are summarized in Table 2 (entry 1). The values of $x^* = (1.6 \pm 0.2)\%$ and $k_p = (2.9 \pm 0.3) \times 10^3$ s^{-1}M^{-1}, in particular, are in nice agreement with the previous literature,[8] and as such represent a validation of our QF setup and protocol.

No significant time evolution of molar mass distribution and ^{13}C NMR microstructure of the nascent polymer was observed (see Table SI-1). The M_w/M_n ratio was large (4–6) from the very beginning, which can be ascribed to the presence of multiple types of catalytic species.[2–4,7–10,32] Notably, the only observed chain ends in the polymers were isobutyl groups (see Figure SI-3), which is consistent with chain initiation at the titanium–isobutyl bonds generated by TIBA, and termination by an acidic quench at last-inserted regioregular 1,2 units (Scheme 2 A). ^{13}C NMR spectra at long accumulation (see Figure SI-4) revealed very low amounts (0.03 %) of isolated 2,1 monomeric units internal to the chains ($k_{ps} = 3 \times 10^{-4}\, k_{pp}$ in Scheme 1). Summing up, it can be concluded that this catalyst system is not dormant, at least in the explored (short) time range.

Table 2: Best-fit values of k_p (average kinetic constant of chain propagation), $\langle f_t \rangle$ (average cumulative frequency of chain transfer), and x^* as measured by QF propene polymerization experiments in a heptane slurry for two different $MgCl_2$-supported catalyst systems (see text).

Entry	ID	ED	T [°C]	k_p [s^{-1} M^{-1}]	x^*	$\langle f_t \rangle$ [s^{-1}]
1	EB	–	30	$(2.9 \pm 0.3) \times 10^3$	0.016 ± 0.002	3 ± 1
2	DIBP	DIBDMSi	40	$(9.4 \pm 0.9) \times 10^3$	0.0021 ± 0.0002	6 ± 1

In present-day industrial i-PP plants, the most commonly used catalysts contain a phthalate ID.[2–4] Compared to those with ID = EB, they feature much more stable kinetics, and a superior stereoselectivity when properly modified with an ED (Table 1). For this study we selected a $MgCl_2/TiCl_4$/DIBP precatalyst (DIBP = diisobutylphthalate) in combination with a TIBA/DIBDMSi cocatalyst (DIBDMSi = diisobutyldimethoxysilane, a common industrial ED[2–4]).

QF investigations of this catalyst class are complicated by slow chain initiation: a recent study demonstrated that it takes several seconds for propene polymerization to take off,[33] which is longer than the initial transient with controlled kinetics. To overcome the problem, we pre-contacted precatalyst and cocatalyst in heptane slurry for 15 minutes at 40 °C in the absence of a monomer, prior to the QF reactions.[34] This protocol turned out to work well, and at 40 °C a linear plot of polymer yield versus time (without any induction) was observed in the 0–0.5 s range (Figure 1). The best-fit values of the main kinetic parameters, obtained by interpolation of the $\{Y, t\}$ and $\{P_n^{-1}, t^{-1}\}$ data sets in the aforementioned time range (Table 3, entries 1–7 and Figure 1), as discussed in Section SI-5.2, are summarized in Table 2 (entry 2). In particular, $k_p = (9.4 \pm 0.9) \times 10^3$ s^{-1}M^{-1} is at the high end of the literature range for ZN catalytic species, whereas $x^* = (0.21 \pm 0.02)\%$ is unusually low.[7–10]

Compared with the EB case, polymer characterizations by ^{13}C NMR spectroscopy and GPC highlighted a drastically different picture (Table 3, entries 1–7 and Figure 2; see also Figures SI-5–SI-7). Particularly revealing are the results of ^{13}C NMR chain-end analysis in Table 3 and Figure 2. Only at very short reaction times ($t < 0.2$ s) did the polymer chains feature predominant terminal isobutyl ends. At longer times butyl ends rapidly built up, and at around $t = 0.3$ s they outnumbered the former. We take these data as a clear indication that a large fraction of the catalytic species in the system has evolved into dormant Ti–CH(Me)–CH$_2$(R) species, which do not undergo further monomer insertion prior to the acidic quench (Scheme 2 D). Along with this, a progressive fade of polymer stereoregularity and broadening of molar

 © 2016 Wiley-VCH Verlag GmbH & Co. KGaA, Weinheim

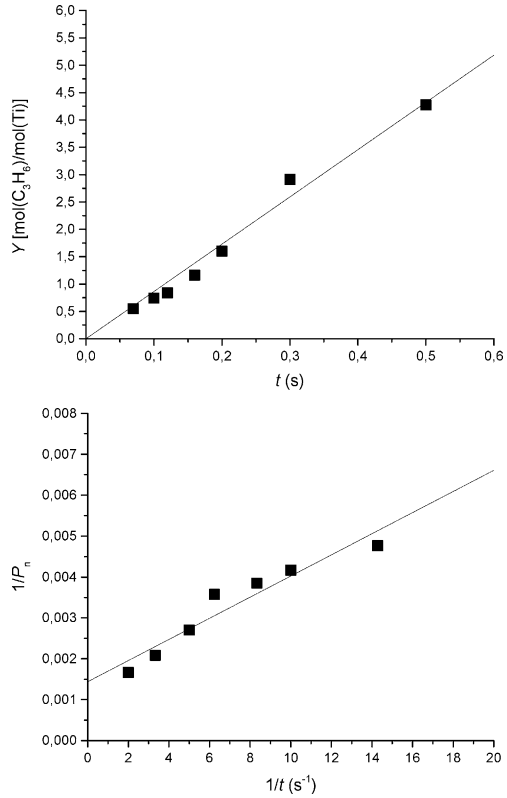

Figure 1. Plots of Y versus t (top) and P_n^{-1} versus t^{-1} (bottom) under controlled regime for propene polymerization in the presence of $MgCl_2/TiCl_4$/DIBP and TIBA/DIBDMSi at 40 °C (Table 3, entries 1–7). For data point interpolation, see Scheme SI-5.2.

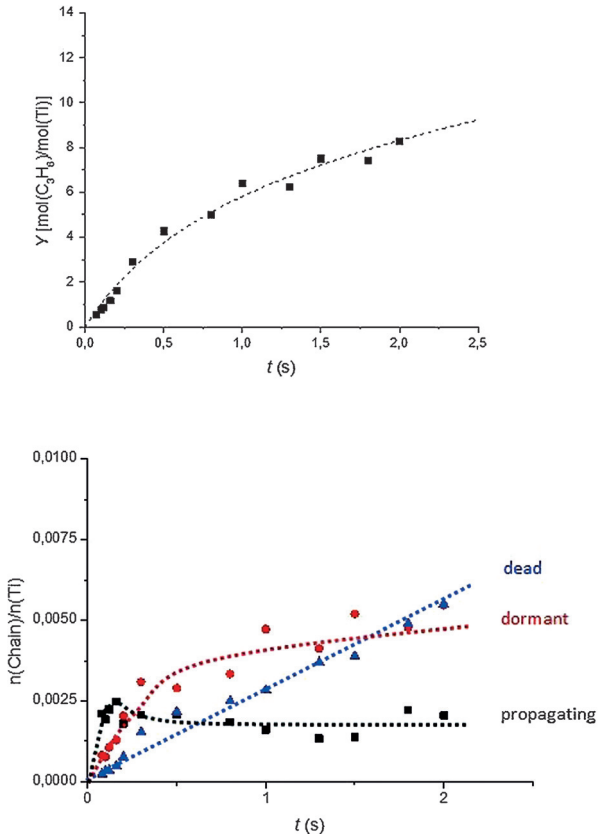

Figure 2. Plots of yield (top) and population distribution of propagating, dormant, and dead (olefin-terminated) chains (bottom) beyond the controlled regime of propene polymerization with $MgCl_2/TiCl_4$/DIBP and TIBA/DIBDMSi at 40 °C. Data from Table 3; the symbols in the bottom plot refer to the chain-end structures in Scheme 2.

mass distribution were revealed by the ^{13}C NMR spectra and GPC traces, respectively (Table 3; see also Figures SI-6 and SI-7).

To better follow the above trends, we extended the QF experiments beyond the duration of the controlled regime (i.e. up to $t = 2$ s). The overall results (Table 3, Figure 2; see also Figures SI-6 and SI-7) highlighted the evolution of the system toward a steady state characterized by a relatively poor productivity and stereoselectivity (both well below commercial standards), and a moderately larger value of x^* (ca. 0.7%) compared with that (0.2%) in the controlled regime.

Table 3: Results of QF propene polymerization experiments in the presence of the catalyst system of $MgCl_2/TiCl_4$/DIBP and TIBA/DIBDMSi at 40 °C (see text and the Supporting Information).

Entry	t [s]	Y[a]	$10^{-2}\,P_n$	M_n [KDa]	M_w/M_n	[*mmmm*][b] [%]	Terminal chain ends (mol%) [isobutyl][c]	[butyl]	[vinylidene][d]
1	0.07	0.55	2.1	8.9	2.9	97.0	0.26	0.13	0.03
2	0.10	0.74	2.4	10.1	3.0	95.8	0.23	0.12	0.02
3	0.12	0.84	2.6	10.9	3.1	95.4	0.23	0.11	0.02
4	0.16	1.16	2.8	11.5	3.4	94.9	0.18	0.10	0.03
5	0.20	1.60	3.7	15.5	4.2	94.5	0.10	0.10	0.04
6	0.30	2.91	4.8	20.2	5.4	94.0	0.04	0.09	0.04
7	0.50	4.27	6.0	25.1	7.1	93.7	0.04	0.05	0.04
8	0.80	5.00	6.5	27.4	7.3	91.9	0.03	0.05	0.03
9	1.00	6.39	7.0	29.3	6.5	91.9	0.02	0.05	0.03
10	1.30	6.25	7.3	30.6	8.2	92.0	0.02	0.05	0.03
11	1.50	7.50	7.2	30.1	7.3	92.5	0.01	0.05	0.04
12	1.80	7.40	7.0	29.6	7.3	90.7	0.02	0.05	0.04
13	2.00	8.26	7.1	29.8	8.6	90.2	0.02	0.05	0.04

[a] [mol(C_3H_6) mol(Ti)$^{-1}$]. [b] Percentage of the isotactic pentad. [c] Estimated as {[isobutyl (total)]−[butyl]}/2. [d] Estimated as [vinylidene] = [propyl]. See Scheme 2.

In our opinion, the above facts indicate that the most active and stereoselective catalytic species in this system are the first to take off, but also those most prone to becoming dormant. This behavior would hamper practical application, were it not for the lucky circumstance that secondary alkyl—titanium species are easily amenable to hydrogenolysis, and H_2 is normally present in propene polymerization reactors as a chain-transfer agent.[2–4] Studying H_2 response requires longer reaction times than those accessible in a QF setup (see Figure SI-8).[35] We carried out a number of propene polymerization experiments in bench reactors under conditions similar to

© 2016 Wiley-VCH Verlag GmbH & Co. KGaA, Weinheim

Table 4: Results of propene polymerization experiments in bench reactors in the presence of the catalyst system $MgCl_2/TiCl_4$/DIBP and TIBA/DIBDMSi at various temperatures and H_2 levels.

Entry	T [°C]	$x(H_2)$ (ν%)[a]	R_p[b]	M_n [KDa]	M_w/M_n	[*mmmm*][c] [%]	Terminal chain ends (mol%) [isobutyl]	[butyl]
1	40	0	9	177	9.1	81.2		
2	40	12	14	22	8.3	88.3	0.13	0.13
3	70	0	39	182	8.4	86.4		
4	70	12	92	22	8.2	94.8	0.08	0.10

For experimental details, see Scheme SI-3. [a] In the gas cap. [b] g(PP) $mg(Ti)^{-1}h^{-1}[C_3H_6]^{-1}$. [c] Percentage of the isotactic pentad.

those of the QF runs, but at a reaction time of 30 minutes (Table 4; entries 1 and 2). In the absence of H_2, catalyst performance turned out to be in line with the QF extrapolation. Indeed, the stationary values of catalyst productivity and polymer ^{13}C NMR stereoregularity extrapolated from the QF data of Table 3 ($R_p = 7$ g(PP) $mg(Ti)^{-1}h^{-1}$ $[C_3H_6]^{-1}$; [*mmmm*] = 82%) compare very well with those measured in the bench experiment ($R_p = 9$ g(PP) $mg(Ti)^{-1}h^{-1}$ $[C_3H_6]^{-1}$; [*mmmm*] = 81.2%; entry 1 of Table 4). This finding is notable, as it indicates that despite the very short duration the QF experiments were representative of catalyst behavior, at least in the examined case.

Adding H_2 at 40 °C caused about a twofold enhancement of catalyst productivity, a clear improvement of polymer ^{13}C NMR stereoregularity, and a sharp decrease of average molar mass, mainly resulting from the hydrogenolysis of secondary alkyl–titanium species, as revealed by the large fraction of terminal butyl chain ends (Table 4, entry 2). All these data are consistent with the re-activation of dormant sites with higher stereoselectivity.[25–27] Not surprisingly, the process is highly activated. As a matter of fact, upon raising the polymerization temperature to 70 °C the trend became much more evident (compare entries 1 and 2 and 3 and 4 of Table 4). In particular, ^{13}C NMR stereoregularity of the i-PP produced at 70 °C in the presence of H_2 (entry 4) ultimately approached that of the nascent polymer isolated at very short reaction time ($t < 0.3$ s) in the QF experiments without H_2 at 40 °C (Table 3, entries 1–6).

The above results conclusively demonstrate that, despite a very high regioselectivity, the self-poisoning of ZN catalysts caused by monomer regioinversion can be severe and is largely responsible for the effects that are comprehensively referred to as hydrogen response.[2–4,25–27]

An important question that needs to be addressed is what determines dormancy for different ZN catalytic species. From the kinetic theory of propene hydro-oligomerization[28] it was concluded that, in a first approximation, the fraction ($x_{rel,d}$*) of dormant sites is given by $x_{rel,d}^* = (1 + k_{sp}/k_{ps})^{-1}$ (Scheme 1). An educated guess is that with increasing steric hindrance at the active metal both k_{ps} and k_{sp} should decrease, but predicting which of the two effects predominates (i.e. the k_{sp}/k_{ps} ratio) is simply not possible without a detailed knowledge of the structure of the catalytic species. This being said, empirically a lower regioselectivity (higher k_{ps}) seems to correlate with higher dormancy: compare ID = EB ($k_{ps} = 3 \times 10^{-4}\, k_{pp}$; see Figure SI-4) with ID = DIBP ($k_{ps} \approx 1.0 \times 10^{-3}\, k_{pp}$; Table 4, entries 2 and 4). The same probably holds for catalysts featuring 1,3-dimethoxypropane IDs ($k_{ps} \approx 3 \times 10^{-3}\, k_{pp}$).[25d] In any case, our results demonstrate how subtle the relationship is between catalyst composition and dormancy.

We find it somehow ironic that H_2, introduced in the 1950s as a most convenient chain-transfer agent with $TiCl_3$-based catalysts to modulate i-PP molar mass,[2–4] was inherited by present-day i-PP production processes without prior understanding of its crucial action on dormant sites. The fortuitous intake of H_2 as a powerful antidote to catalyst self-poisoning must then be added to the already long list of astonishingly lucky finds behind the success of this fascinating catalysis.[4]

Keywords: alkenes · hydrogen · kinetics · NMR spectroscopy · polymerization

How to cite: *Angew. Chem. Int. Ed.* **2016**, *55*, 8590–8594
Angew. Chem. **2016**, *128*, 8732–8736

[1] S. Ali, *Catal. Rev.* **2014**, *27*, 7.
[2] G. Cecchin, G. Morini, F. Piemontesi in *Kirk-Othmer Encyclopedia of Chemical Technology, 5th* ed., *Vol. 26* (Ed.: A. Seidel), Wiley, Hoboken, **2007**, p. 502.
[3] *Polypropylene Handbook* (Ed.: E. P. Moore, Jr.), Hanser-Gardner Publications, Cincinnati, **1996**.
[4] "Polyolefins: 50 years after Ziegler and Natta [Vol. I] (Ed.: W. Kaminsky)" *Adv. Polym. Sci.* **2013**, *257*.
[5] A. Zambelli, P. Locatelli, G. Bajo, F. A. Bovey, *Macromolecules* **1975**, *8*, 687–689.
[6] V. Busico, R. Cipullo, *Prog. Polym. Sci.* **2001**, *26*, 443–533.
[7] a) T. Keii, M. Terano, K. Kimura, K. Ishii, *Makromol. Chem. Rapid Commun.* **1987**, *8*, 583–587; b) M. Terano, T. Kataoka, T. Keii, *J. Mol. Catal.* **1989**, *56*, 203–210.
[8] H. Mori, H. Iguchi, K. Hasebe, M. Terano, *Macromol. Chem. Phys.* **1997**, *198*, 1249–1255.
[9] a) M. Mori, M. Terano, *Trends Polym. Sci.* **1997**, *5*, 314–321; b) B. P. Liu, H. Matsuoka, M. Terano, *Macromol. Rapid Commun.* **2001**, *22*, 1–24.
[10] T. Taniike, S. Sano, M. Ikeya, V. Q. Thang, M. Terano, *Macromol. React. Eng.* **2012**, *6*, 275–279.
[11] V. Busico, G. Talarico, R. Cipullo, *Macromol. Symp.* **2005**, *226*, 1–16.
[12] A. K. Yaluma, P. J. T. Tait, J. C. Chadwick, *J. Polym. Sci. Part A* **2006**, *44*, 1635–1647.
[13] J. Mejzlik, M. Lesna, J. Kratochvila, *Adv. Polym. Sci.* **1986**, *81*, 83–120.
[14] J. C. W. Chien, C.-I. Kuo, *J. Polym. Sci. Part A* **1985**, *23*, 731–760.
[15] V. Busico, M. Guardasole, A. Margonelli, A. L. Segre, *J. Am. Chem. Soc.* **2000**, *122*, 5226–5227.
[16] N. Bahri-Laleh, A. Correa, S. Mehdipour-Ataei, H. Arabi, M. N. Haghighi, G. Zohuri, L. Cavallo, *Macromolecules* **2011**, *44*, 778–783.
[17] J. C. W. Chien, Y. Hu, *J. Polym. Sci. Part A* **1989**, *27*, 897–913.
[18] E. Morra, E. Giamello, S. Van Doorslaer, G, Antinucci, M. D'Amore, V. Busico, M. Chiesa, *Angew. Chem. Int. Ed.* **2015**, *54*, 4857–4860; *Angew. Chem.* **2015**, *127*, 4939–4942.
[19] See, for example: E. Groppo, E. Gallo, K. Seenivasan, K. A. Lomachenko, A. Sommazzi, S. Bordiga, P. Glatzel, R. van Silfh-

 © 2016 Wiley-VCH Verlag GmbH & Co. KGaA, Weinheim

out, A. Kachatkou, W. Bras, C. Lamberti, *ChemCatChem* **2015**, *7*, 1432 – 1437.
[20] a) F. Auriemma, V. Busico, P. Corradini, M. Trifuoggi, *Eur. Polym. J.* **1992**, *28*, 513; b) V. Busico, P. Corradini, L. De Martino, M. Trifuoggi, *Eur. Polym. J.* **1992**, *28*, 519 – 523.
[21] V. Busico, R. Cipullo, G. Monaco, G. Talarico, M. Vacatello, J. C. Chadwick, A. L. Segre, O. Sudmeijer, *Macromolecules* **1999**, *32*, 4173 – 4182.
[22] T. Taniike, M. Terano, *J. Catal.* **2012**, *293*, 39 – 50.
[23] a) Z. Zhoua, R. Kümmerle, J. C. Stevens, D. Redwinec, Y. Hec, X. Qiuc, R. Conga, J. Klosin, N. Montañez, G. Roof, *J. Magn. Reson.* **2009**, *200*, 328 – 333; b) Z. Zhou, J. C. Stevens, J. Klosin, R. Kümmerle, X. Qiu, D. Redwine, R. Cong, A. Taha, J. Mason, B. Winniford, P. Chauvel, N. Montañez, *Macromolecules* **2009**, *42*, 2291 – 2294.
[24] V. Busico, R. Cipullo, A. Mingione, L. Rongo, *Ind. Eng. Chem. Res.* **2016**, in press.
[25] a) V. Busico, R. Cipullo, G. Talarico, L. Caporaso, *Macromolecules* **1998**, *31*, 2387 – 2390; b) V. Busico, R. Cipullo, S. Ronca, *Macromolecules* **2002**, *35*, 1537 – 1542; c) V. Busico, R. Cipullo, C. Polzone, G. Talarico, J. C. Chadwick, *Macromolecules* **2003**, *36*, 2616 – 2622; d) V. Busico, J. C. Chadwick, R. Cipullo, S. Ronca, G. Talarico, *Macromolecules* **2004**, *37*, 7437 – 7443.
[26] V. Busico, R. Cipullo, J. C. Chadwick, J. F. Modder, O. Sudmeijer, *Macromolecules* **1994**, *27*, 7538 – 7543.
[27] a) J. C. Chadwick, G. M. Van Kessel, O. Sudmeijer, *Macromol. Chem. Phys.* **1995**, *196*, 1431 – 1437; b) J. C. Chadwick, G. Morini, E. Albizzati, G. Balbontin, I. Mingozzi, A. Cristofori, O. Sudmeijer, G. M. M. Van Kessel, *Macromol. Chem. Phys.* **1996**, *197*, 2501 – 2510; c) J. C. Chadwick, F. P. T. J. van der Burgt, S. Rastogi, V. Busico, R. Cipullo, G. Talarico, J. J. R. Heere, *Macromolecules* **2004**, *37*, 9722 – 9727.
[28] V. Busico, R. Cipullo, P. Corradini, *Makromol. Chem.* **1993**, *194*, 1079 – 1093.
[29] C. R. Landis, D. R. Sillars, J. M. Batterton, *J. Am. Chem. Soc.* **2004**, *126*, 8890 – 8891.
[30] V. Busico, R. Cipullo, V. Romanelli, S. Ronca, M. Togrou, *J. Am. Chem. Soc.* **2005**, *127*, 1608 – 1609.
[31] $AlEt_3$ (TEA) is the most commonly used cocatalyst in $MgCl_2$-supported ZN catalysis. However, it can produce ethene by β-hydride elimination, which may perturb propene polymerization kinetics under QF conditions, as we verified in preliminary experiments. Therefore, we decided to use TIBA. Release of isobutene by β-hydride elimination, which also occurs, is immaterial because isobutene is practically unreactive with ZN catalytic species.
[32] Y. V. Kissin, R. Ohnishi, T. Konakazawa, *Macromol. Chem. Phys.* **2004**, *205*, 284 – 301.
[33] S. Dwivedi, T. Taniike, M. Terano, *Macromol. Chem. Phys.* **2014**, *215*, 1698 – 1706.
[34] a) H. Mori, M. Yamahiro, M. Terano, M. Takahashi, T. Matsukawa, *Macromol. Chem. Phys.* **2000**, *201*, 289 – 295; b) T. Nitta, B. P. Liu, H. Nakatani, M. Terano, *J. Mol. Catal. A* **2002**, *180*, 25 – 34.
[35] a) H. Mori, K. Tashino, M. Terano, *Macromol. Rapid Commun.* **1995**, *16*, 651 – 657; b) B. P. Liu, N. Murayama, M. Terano, *Ind. Eng. Chem. Res.* **2005**, *44*, 2382 – 2388.

Received: March 10, 2016
Published online: May 31, 2016

 © 2016 Wiley-VCH Verlag GmbH & Co. KGaA, Weinheim